

## Heat transfer enhancement in natural convection in micropolar nanofluids

K. RUP, K. NERING

*Faculty of Mechanical Engineering  
Cracow University of Technology  
Jana Pawła II 37  
31-864 Kraków, Poland  
e-mails: krup@usk.pk.edu.pl, knering@mech.pk.edu.pl*

IN THIS WORK AN ANALYSIS OF MOMENTUM, ANGULAR MOMENTUM and heat transfer during unsteady natural convection in micropolar nanofluids is presented. Selected nanofluids treated as single phase fluids, contain small particles. In particular, two ethylene glycol-based nanofluids were analyzed. The volume fraction of these solutions was 6%, 3.5% and 0.6%. The first ethylene glycol solution contained  $\text{Al}_2\text{O}_3$  nanoparticles ( $d = 38.4$  nm), and the second ethylene glycol solution contained Cu nanoparticles ( $d = 10$  nm).

**Key words:** micropolar fluid, nanofluid, heat transfer enhancement.

Copyright © 2016 by IPPT PAN

### Notations

$\rho$	density, $\text{kg/m}^3$ ,
$d_p$	diameter of the nanoparticle, nm,
$\mu_v$	dynamic viscosity, $\text{Pa} \cdot \text{s}$ ,
$\nu_\infty$	kinematic viscosity $\nu_\infty = (\mu_v/\rho)_\infty$ , $\text{m}^2/\text{s}$ ,
$k_b$	Boltzmann constant, $\text{J/K}$
$t$	temperature, K,
$c$	specific heat at constant pressure of nanofluid,
$M$	molecular weight of base fluid,
$N_A$	Avogadro number,
$\beta$	coefficient of thermal expansion, $1/\text{K}$
$\tau$	time, s
$u, v$	components of velocity field, $\text{m/s}$ ,
$\kappa_v$	rotational viscosity coefficient, $\text{Pa} \cdot \text{s}$ ,
$\mathbf{v}_r^{(z)}$	microrotation component normal to $(x, y)$ -plane, $1/\text{s}$ ,
$\gamma_v$	spin gradient viscosity, $\text{N} \cdot \text{s}$ ,
$j$	microinertia density, $\text{m}^2$ ,
$a$	fluid thermal diffusivity, $\text{m}^2/\text{s}$ ,
$P, \Delta$	dimensionless micropolar fluid parameters,
$q_0$	constant heat flux through the vertical plate,
$K$	total number of spatial steps in $x$ directions,
$L$	total number of spatial steps in $y$ directions,

$\tau_w$  shear stress of a vertical surface, Pa,  
 $\lambda$  thermal conductivity, W/(m · K),  
 $T$  dimensionless temperature,  
 $\varphi$  nanoparticle volume fraction.

Subscripts

$f$  refers to properties of base fluid,  
 $f_0$  refers to properties of base fluid at temperature 293K,  
 $s$  refers to properties of solid nanoparticles.

## 1. Introduction

CONVENTIONAL FLUIDS THAT ARE WIDELY USED in heat exchange devices, such as water, oil, alcohol, and glycol ethylene, have a relatively low thermal conductivity coefficient. Recently, a new generation of heat carriers known as nanofluids has been developed [1]–[4]. These types of fluids consist of conventional fluid and nanoparticles with particle diameters between 10 and 100 nm mixed uniformly with fluid. Generally, they contain particles of substances such as Al<sub>2</sub>O<sub>3</sub>, TiO<sub>2</sub>, CuO and Cu [1, 4]. The discussed nanofluids are characterized by increased effective thermal conductivity and dynamic viscosity. During experimental studies, the nanofluids behave like a single phase Newtonian fluid in the convective heat exchange process [2]–[5]. Recently, methods presented in the literature [4, 5] which were based on large numbers of experimental data were used to determine the thermophysical parameters of nanofluids. These correlations provide theoretical and practical analysis of heat exchange due to natural convection. One paper [1] analyzes the process of steady natural convection in nanofluid in the vicinity of a vertical plate heated by constant heat flux. In particular, the water suspension of Al<sub>2</sub>O<sub>3</sub> and CuO was analyzed. The volume fraction of these suspensions did not exceed 10%. Similar work [2] described natural convection in the water suspension of Al<sub>2</sub>O<sub>3</sub> with the same thermodynamic conditions. Another paper [3] describes the numerical solution of equations of conservation of mass, momentum and energy in the natural convection process in the water suspensions of Al<sub>2</sub>O<sub>3</sub> and CuO placed in six different closed areas. Increased heat exchange was observed only in the triangle-shaped area. The amount of increase was only 5% compared to water without nanoparticles [3].

Due to the miniaturization of heat exchange devices, micropolar fluids as refrigerant or heating media are also analyzed in the literature [6]–[8]. A useful model of micropolar fluid is the model proposed by Eringen [6]. This model takes into account fluid microrotation [6]–[8].

The aim of the work described in this paper is the analysis of increased heat exchange due to natural unsteady convection in ethylene glycol solutions of Al<sub>2</sub>O<sub>3</sub> and Cu with properties of micropolar nanofluids in the vicinity of a vertical plate heated by heat flux of  $q_0$  that rises suddenly.

## 2. Estimating properties of nanofluids

The typical approach used to study the thermodynamic properties of nanofluids is based on the assumption that nanofluids behave like single phase fluids. There are empirical equations, proposed by the authors, which are used to determine different features of nanofluids such as thermal conductivity, viscosity, density and thermal expansion [4, 5]. It is worth mentioning that all the models are applicable only in specific range of nanofluid parameters.

Several authors are proposing different methods to estimate the heat conductivity of nanofluid. This parameter is the most important with respect to the heat transfer process [4, 5]. Based on the large amount of data presented in [4], a method of heat conductivity calculation was proposed:

$$(2.1) \quad \lambda = \lambda_f + 4.4 \cdot \text{Re}^{0.4} \cdot \text{Pr}_f^{0.66} \cdot \left( \frac{t}{t_{fr}} \right)^{10} \cdot \lambda_f \cdot \left( \frac{\lambda_s}{\lambda_f} \right)^{0.03} \cdot \varphi^{0.66}.$$

Equation (2.1) is suggested especially when nanofluid is based on water and glycol ethylene with  $\text{Al}_2\text{O}_3$ ,  $\text{TiO}_2$ ,  $\text{CuO}$  or  $\text{Cu}$  nanoparticles. In Eq. (2.1), the Reynolds number is given by the equation defined for nanofluids in [4]:

$$(2.2) \quad \text{Re} = \frac{2 \cdot \rho_f \cdot k_b \cdot t}{\pi \cdot \mu_f^2 \cdot d_p}$$

and the Prandtl number is:

$$(2.3) \quad \text{Pr} = \frac{\mu_v \cdot (c \cdot \rho)}{\lambda \cdot \rho}.$$

Equation (2.3) shows that the Prandtl number increases after adding nanoparticles to the base fluid.

Many models determining dynamic viscosity have been developed [5]. For example, classic models such as Einstein's (2.4) or Brinkman's (2.5) models:

$$(2.4) \quad \mu_v = (1 + 2.5 \cdot \varphi) \cdot \mu_f,$$

$$(2.5) \quad \mu_v = \frac{\mu_f}{(1 - \varphi)^{2.5}}.$$

For the water suspension of the nanoparticles of  $\text{Al}_2\text{O}_3$ , the authors recommend the following relationship [4]:

$$(2.6) \quad \mu_v = (123 \cdot \varphi^2 + 7,3 \cdot \varphi + 1) \cdot \mu_f.$$

Recently, using a large amount of experimental data from many authors, an empirical equation to determine dynamic viscosity has been proposed [4]:

$$(2.7) \quad \mu_v = \frac{\mu_f}{1 - 34.87(d_p/d_f)^{-0.3} \cdot \varphi^{1.03}}.$$

To calculate the equivalent diameter of a base fluid molecule from equation (2.7), an equation proposed by [4] was used:

$$(2.8) \quad d_f = \frac{6 \cdot M}{N_A \cdot \pi \cdot \rho_{f0}}.$$

One of the methods to determine the density, heat capacity and thermal expansion coefficient is the conventional approach [4, 5]. It can be assumed that nanofluid is a single phase fluid. Thus, those parameters can be calculated as in the case of mixtures. It is given by:

$$(2.9) \quad \rho = (1 - \varphi) \cdot \rho_f + \varphi \cdot \rho_s,$$

$$(2.10) \quad \rho c = (1 - \varphi) \cdot (\rho c)_f + \varphi \cdot (\rho c)_s,$$

$$(2.11) \quad \rho \beta = (1 - \varphi) \cdot (\rho \beta)_f + \varphi \cdot (\rho \beta)_s.$$

In energy equations, the heat capacity and thermal expansion coefficient are always considered with fluid density; thus Eqs. (2.10) and (2.11) will be used.

### 3. Problem formulation

The field equations of the micropolar fluids are [6]:

$$(3.1) \quad \frac{\partial \rho}{\partial \tau} + (\rho v_k)_{,k} = 0,$$

$$(3.2) \quad -\boldsymbol{\pi}_{,k} + (\lambda + \mu_v) v_{l,kl} + (\mu_v + \kappa_v) v_{k,ll} + \kappa_v \epsilon_{klm} \nu_{m,l} + \rho(f_k - \dot{v}_k) = 0,$$

$$(3.3) \quad (\alpha_v + \beta_v) \nu_{l,kl} + \gamma_v \nu_{k,ll} + \kappa_v \epsilon_{klm} \nu_{m,l} - 2\kappa_v \nu_k + \rho(l_k - j \dot{\nu}_k) = 0,$$

$$(3.4) \quad \rho \dot{\epsilon} = t_{kl} d_{lk} + t_{kl} \epsilon_{klr} (\omega_r - \nu_r) + m_{kl} \nu_{l,k} + q_{k,k} + \rho h,$$

$$(3.5) \quad \dot{v}_k \equiv \frac{\partial v_k}{\partial \tau} + v_{k,l} v_l, \quad \dot{\nu}_k \equiv \frac{\partial \nu_k}{\partial \tau} + \nu_{k,l} \nu_l.$$

In the above equations  $\epsilon_{klr}$  is the alternating tensor. The axial vector  $\mathbf{v}_r$  will be called microrotation vector. Thermodynamic pressure  $\boldsymbol{\pi}$  is defined in [6] by  $\boldsymbol{\pi} \equiv -\frac{\partial \epsilon}{\partial \rho^{-1}}|_{\eta,i}$ .

In this paper unsteady laminar momentum, angular momentum and heat exchange in micropolar nanofluids in terms of natural convection will be considered. Micropolar nanofluid is in the vicinity of a vertical plate. The heat flux through the plate rises suddenly to the value of  $q_0$ .

The problem presented in this work will be solved using the following assumptions:

- the Oberbeck–Boussinesq approximation is assumed;
- the geometry of the analyzed flows justifies the use of the boundary layer theory;

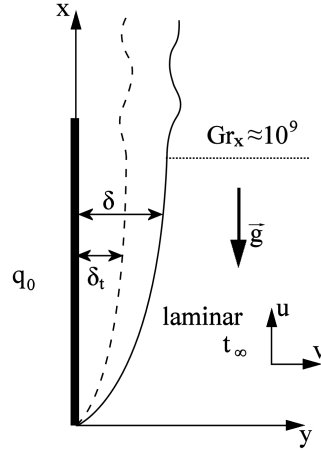


FIG. 1. Considered fluid schema.

- the viscous dissipation and pressure work are neglected;
- Eringen's theory of thermomicrofluid is assumed.

Taking into account the simplification resulting from the boundary layer theory and fluid density changes according to the Oberbeck–Boussinesq approximation the following system of equations can be obtained:

$$(3.6) \quad \frac{\partial u}{\partial x} + \frac{\partial v}{\partial y} = 0,$$

$$(3.7) \quad \frac{\partial u}{\partial \tau} + u \frac{\partial u}{\partial x} + v \frac{\partial u}{\partial y} = \frac{1}{\rho} (\mu_v + \kappa_v) \frac{\partial^2 u}{\partial y^2} + \frac{\kappa_v}{\rho} \frac{\partial \mathbf{v}_r^{(z)}}{\partial y} + g\beta(t - t_\infty),$$

$$(3.8) \quad \frac{\partial \mathbf{v}_r^{(z)}}{\partial \tau} + u \frac{\partial \mathbf{v}_r^{(z)}}{\partial x} + v \frac{\partial \mathbf{v}_r^{(z)}}{\partial y} = \frac{\gamma_v}{\rho j} \frac{\partial^2 \mathbf{v}_r^{(z)}}{\partial y^2} - \frac{\kappa_v}{\rho j} \left( 2\mathbf{v}_r^{(z)} + \frac{\partial u}{\partial y} \right),$$

$$(3.9) \quad \frac{\partial t}{\partial \tau} + u \frac{\partial t}{\partial x} + v \frac{\partial t}{\partial y} = a \frac{\partial^2 t}{\partial y^2}.$$

The above system of partial differential equations together with the following boundary conditions:

$$(3.10) \quad \tau < 0, \quad u = v = 0, \quad t = t_\infty,$$

$$(3.11) \quad \tau \geq 0, \quad x = 0, \quad u = v = 0, \quad t = t_\infty,$$

$$(3.12) \quad y = 0, \quad u = v = 0, \quad \frac{\partial t}{\partial y} = -\frac{q_0}{\lambda}, \quad \mathbf{v}_r^{(z)} = -n \frac{\partial u}{\partial y},$$

$$(3.13) \quad y \rightarrow \infty, \quad u = 0, \quad \mathbf{v}_r^{(z)} = 0, \quad t = t_\infty,$$

formulates the mathematical description of momentum, angular momentum and heat transfer driven by the unsteady convection in micropolar nanofluids.

In Eqs. (3.6) to (3.9),  $u$  and  $v$  are the velocity components in the  $x$  and  $y$  directions,  $\mathbf{v}_r^{(z)}$  is the microrotation component in the  $xy$ -plane,  $\tau$  the time,  $\rho$  the density,  $\mu_v$  the dynamic viscosity,  $\kappa_v$  the rotational viscosity coefficient,  $\gamma_v$  the spin-gradient viscosity,  $j$  the microinertia density,  $a$  the thermal diffusivity,  $\beta$  the coefficient of volumetric expansion and  $t$  the fluid temperature. In the present analysis, the spin gradient viscosity is assumed to be [7, 8]:

$$(3.14) \quad \gamma_v = \left( \mu_v + \frac{\kappa_v}{2} \right) j.$$

In the condition listed in (3.12) we have assumed that the microcirculation on the boundary layer is equal to the angular velocity, namely,

$$\mathbf{v}_r^{(z)}(x, 0, \tau) = -n \frac{\partial u}{\partial y}.$$

As the suspended particle cannot get closer than its radius to the wall, the microstructure effect must be negligible on the boundary. Therefore, in the vicinity of the boundary, the rotation is due to fluid shear and thus the microrotation must be equal to the angular velocity of the boundary.

In condition (3.12), the parameter  $n$  is a number between 0 and 1 that relates microgyration vector to the shear stress. The value  $n = 0$  corresponds to a high density of liquid microparticles that prevents them from performing rotational movements in the vicinity of the wall. The value  $n = 0.5$  is indicative of weak concentrations; at  $n = 1$  flows, are believed to represent turbulent boundary layers [7, 8].

The fluid differential equations are recast in a dimensionless form by introducing:

$$(3.15) \quad T = \frac{t - t_\infty}{[\nu_\infty^2 (\frac{q}{\lambda})^3 \frac{1}{g\beta}]^{1/4}}, \quad \bar{\tau} = \frac{\tau}{[(\frac{\lambda}{q_0}) \frac{1}{g\beta}]^{1/2}},$$

$$(3.16) \quad U = \frac{u}{[\nu_\infty^2 \frac{q_0}{\lambda} g\beta]^{1/4}}, \quad V = \frac{v}{[\nu_\infty^2 \frac{q_0}{\lambda} g\beta]^{1/4}},$$

$$(3.17) \quad X = \frac{x}{[\nu_\infty^2 \frac{\lambda}{q_0} \frac{1}{g\beta}]^{1/4}}, \quad Y = \frac{y}{[\nu_\infty^2 \frac{\lambda}{q_0} \frac{1}{g\beta}]^{1/4}} = \frac{y}{x} (\text{Gr}_x)^{1/4},$$

$$(3.18) \quad \text{Gr}_x = \frac{g\beta}{\nu_\infty^2} \frac{q_0}{\lambda} x^4, \quad \overline{\mathbf{v}_r^{(z)}} = \mathbf{v}_r^{(z)} \left[ g\beta \frac{q_0}{\lambda} \right]^{-1/2},$$

$$(3.19) \quad \Delta = \frac{\kappa_v}{\nu_\infty \rho}, \quad P = \frac{\nu_\infty}{j} \frac{1}{(\frac{q_0}{\lambda} g\beta)^{1/2}} = \frac{x^2}{j} (\text{Gr}_x)^{-1/2}.$$

The set of partial differential equations (3.6)–(3.9), together with the initial and boundary conditions (3.10)–(3.13) in dimensionless form, will be solved numerically using the finite difference method [8, 9].

#### 4. Problem solution

Equations (3.6)–(3.9) in dimensionless form will be solved using the explicit finite difference scheme. The spatial distribution grid contains  $K \times L$  points in the  $X$  and  $Y$  directions, respectively, and  $\Delta\bar{\tau}$  is the dimensionless time step. Due to the intensive heat, momentum, angular momentum and mass transfer, only in the direct vicinity of the considered vertical surface, the maximum values of the dimensionless coordinates  $X = 100$  and  $Y = 30$  were assumed [8]. A characteristic feature of the difference equations was to determine the temperature field, the velocity field components and the microrotation component  $\overline{\mathbf{v}}_r^{(z)}$  at time  $\bar{\tau}_{n+1}$  depending on certain parameters, but determined at time  $\bar{\tau}_n$ . The convection terms of balance equations comprising time  $\bar{\tau}$  derivatives and spatial  $Y$  coordinate derivatives were approximated by “forward” formulas, whereas spatial  $X$  coordinate derivatives were approximated by “backward” formulas. Diffusion terms were approximated by central differences. Derivatives appearing in the boundary conditions (3.12) were approximated by higher order difference formulas taken in the form [9]:

$$(4.1) \quad \frac{\partial T}{\partial Y|_{ij}} = \frac{1}{6\Delta Y}(-11T_{ij} + 18T_{i,j+1} - 9T_{i,j+2} + 2T_{i,j+3}) + O[\Delta Y]^3,$$

$$(4.2) \quad -\frac{1}{n} \overline{\mathbf{v}}_r^{(z)}|_{i,j} = \frac{\partial U}{\partial Y|_{ij}} = \frac{1}{12\Delta Y}(-25U_{i,j} + 48U_{i,j+1} - 36U_{i,j+2} + 16U_{i,j+3} - 3U_{i,j+4}) + O[\Delta Y]^4.$$

These difference formulas are statically stable and exhibit characteristics of conservation [9].

Before performing basic calculations for the established, non-zero values of parameters  $\Delta$  and  $P$  describing the properties of micropolar fluid, calculation tests were done similarly to [8]. In the process of steady natural convection in a Newtonian fluid, exact analytical solutions are known [10], and were compared to the corresponding calculation results. On the basis of trial calculations, further ones taking into account the non-zero values of  $\Delta$  and  $P$  parameters were performed with the following spatial area division:  $K \times L = 250 \times 150$ , the set dimensionless time step size  $\Delta\bar{\tau} = 0.002$ . The assumed area division is smaller than the area division in work [8] and the time step is two times greater. This change of area division and time step needs to be done to obtain greater accuracy for the applied differential forms.

## 5. Results and discussion

The set of Eqs. (3.6)–(3.9) with the initial condition (3.10) and boundary conditions (3.11)–(3.13) were integrated for the selected values of parameters  $Pr_\infty$ ,  $P$ ,  $\Delta$  and  $n$ . Ethylene glycol (G) in temperature of  $60^\circ\text{C}$  was the base fluid. The Prandtl number of the base fluid was  $Pr_\infty = 56.310$ . In the next stage of the analysis it was assumed that the base fluid has micropolar features with the following parameters:  $\Delta = 5.0$ ,  $P = 1.0$  and  $n = 0.5$ . These parameters were assumed based on the literature and the authors' previous work [8].

The main analysis was focused on the effects occurring in nanofluids. In this work, the following homogeneous ethylene glycol solutions of nanoparticles were analyzed:

- the ethylene glycol solution of  $\text{Al}_2\text{O}_3$  nanoparticles with a mean diameter of 38.4 nm (G +  $\text{Al}_2\text{O}_3$ );
- the ethylene glycol solution of Cu nanoparticles with a mean diameter of 10 nm (G + Cu).

The nanoparticle volume fraction for the above solutions was  $\varphi$ : 6%, 3.5% and 0.6%. The parameters describing these solutions for the temperature of  $60^\circ\text{C}$ , which were calculated using Eqs. (2.1)–(2.11) were presented in Table 1.

**Table 1. Thermophysical parameters of water-based nanofluids in the temperature  $t_\infty = 60^\circ\text{C}$ .**

Fluid	density $\rho$ [kg/m <sup>3</sup> ]	dynamic viscosity $\mu_v$ $10^{-3}$ [kg/(m s)]	thermal conductivity $\lambda$ [W/(m K)]	heat capacity $\rho c_p$ [Jm <sup>3</sup> /K]	thermal expansion $\rho\beta$ [kg/(K · m <sup>3</sup> )]	Prandtl number $Pr_\infty$	normalized coordinates $X/X_f$ ; $Y/Y_f$	normalized parameter $\Delta/\Delta_f$	normalized parameter $P/P_f$
Ethylene glycol (G) $\varphi = 0\%$	1088.1	5.706	0.2598	2789779.6	0.6202	56.310	1.000	1.000	1.000
G + $\text{Al}_2\text{O}_3$ (38.4 nm) $\varphi = 6\%$	1255.61	12.47	0.4630	2800485.0	0.5850	60.052	0.598	0.458	2.798
G + Cu (10 nm) $\varphi = 6\%$	1559.21	30.39	0.633	2828907.0	0.6104	87.180	0.378	0.188	6.999
G + Cu (10 nm) $\varphi = 0.6\%$	1135.21	6.174	0.3413	2793692.3	0.6192	44.520	0.907	0.924	1.220
G + Cu (10 nm) $\varphi = 3.5\%$	1362.92	10.69	0.5209	2812603.8	0.6145	42.350	0.648	0.534	2.380

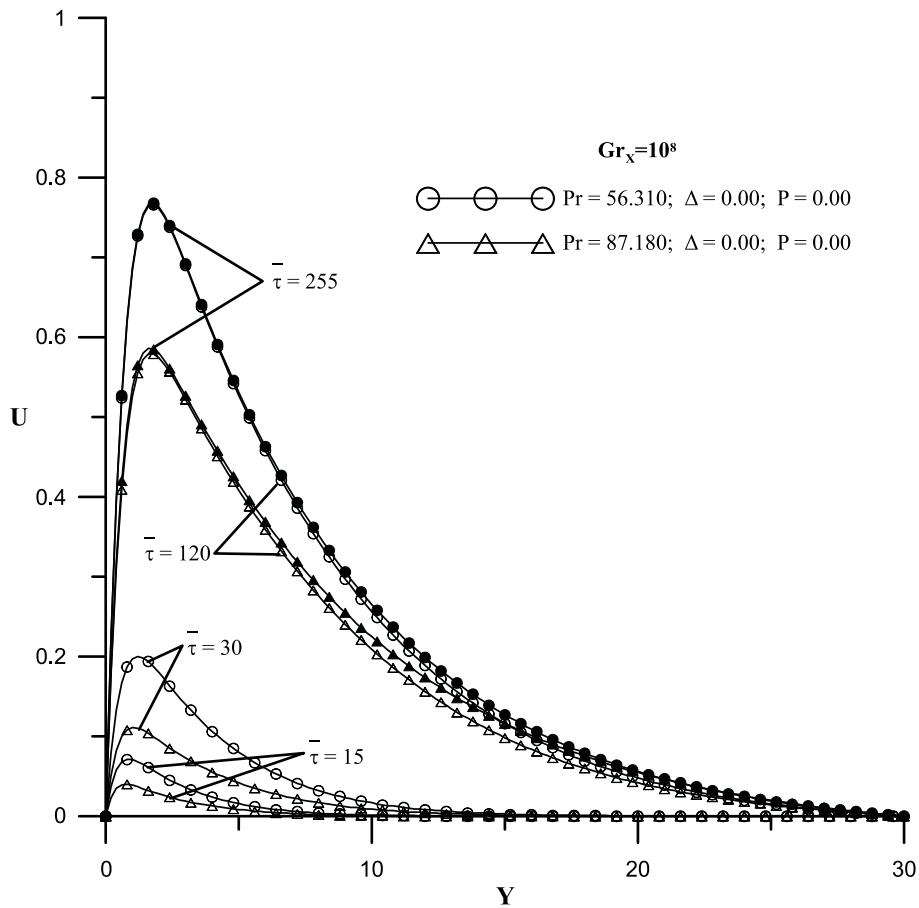


FIG. 2. Profiles of the velocity component  $U$  at selected moments of the process.

Figure 2 shows the dimensionless  $U$  velocity component in the  $X$ -axis direction of the ethylene glycol ( $Pr_\infty = 56.310$ ) and nanofluids with the Prandtl number  $Pr_\infty = 87.180$  at fixed times of the process  $\bar{\tau} = 15, 30, 120$  and  $255$ . In order to simplify the analysis of the thermophysical parameters values of  $\Delta$  and  $P$  were considered to equal zero. Figure 2 shows two different cases with the characteristic value of the Grashof number  $Gr_x = 10^8$ . For the assumed Grashof number, the dimensionless coordinate  $X$  adopts values from Table 1. For nanofluids ( $G + Cu$ ), this  $X$  value equals  $X^{Cu} = 0.378X_f$ . The lines marked with circles represent the results for pure ethylene glycol as the base fluid. The lines marked with triangles represent the results of velocity component  $U$  in nanofluids. Additionally, to obtain an unambiguous description, the  $U$  component of the velocity profiles obtained for the process of  $\bar{\tau} = 255$  is marked with black symbols. The maximum values of velocity component  $U$  in nanofluids are

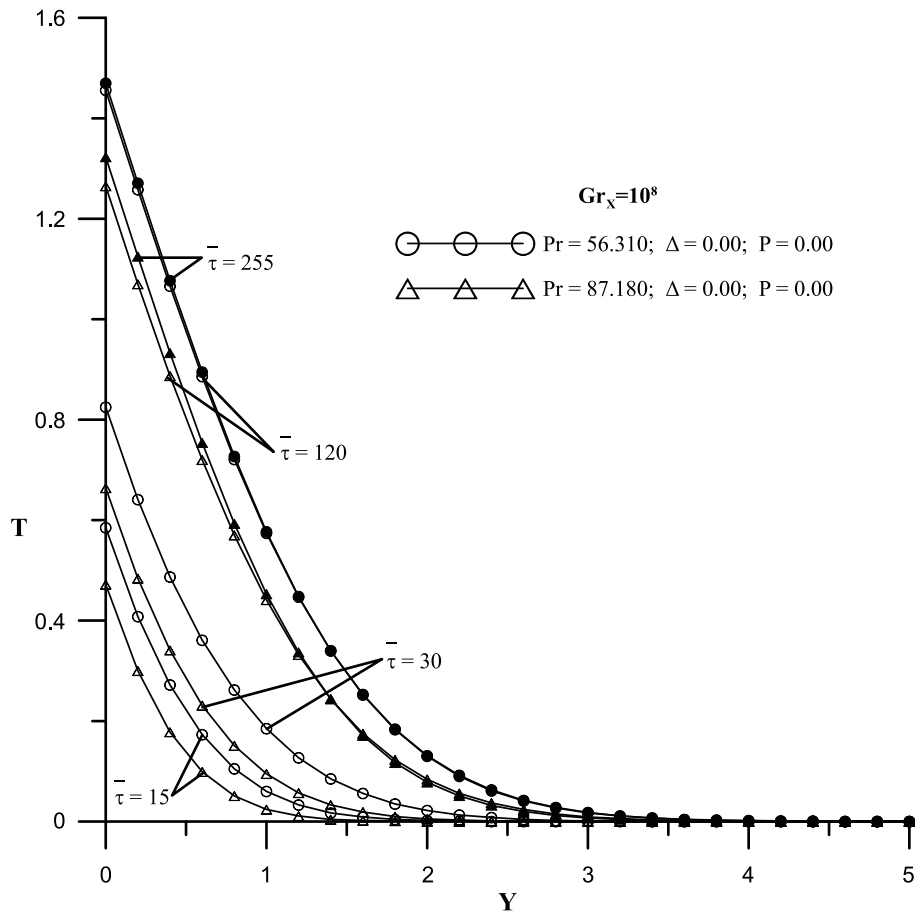


FIG. 3. Profiles of the fluid temperature changes.

lower than the correspondent values for pure ethylene glycol, especially at the initial times of heating.

Figure 3 presents the temperature profiles in the considered liquids at certain moments of the process  $\bar{\tau} = 15, 30, 120$  and  $255$ . Similarly, as for the  $U$  velocity component, the proper values of parameters describing the thermophysical properties of the fluid were assumed. The temperature of the heated plate is lower for fluid with nanoparticles ( $\Delta = 0$ ;  $P = 0$ ). The maximal relative decrease in temperature of the heated plate for nanofluids in the last stage of the process is  $\sigma_{Cu} = (T_s - T_s^f)/T_s^f = -0.198$ . The lower temperature of the heated vertical plate indicates a significantly larger intensity of heat transfer by the analyzed nanofluids than by the pure ethylene glycol. Figure 3 shows a larger rate of heat transfer intensity in nanofluids in the entire range of time in comparison with pure ethylene glycol.

On the basis of the temperature profile, the specified changes in the local Nusselt number  $Nu_x$  in the analyzed fluid on the heated vertical plate are:

$$(5.1) \quad Nu_x = \frac{q_0}{t_w - t_\infty} \frac{x}{\lambda}.$$

Using dimensionless equations (3.14)–(3.18) with the Nusselt number (5.1) we obtain:

$$(5.2) \quad \frac{Nu_x}{Gr_x^{1/5}} = X^{1/5} \frac{1}{T_w},$$

where

$$(5.3) \quad T_w = \frac{t_w - t_\infty}{\left[ \nu_\infty^2 \left( \frac{q_0}{\lambda} \right)^3 \frac{1}{g\beta} \right]^{1/4}}.$$

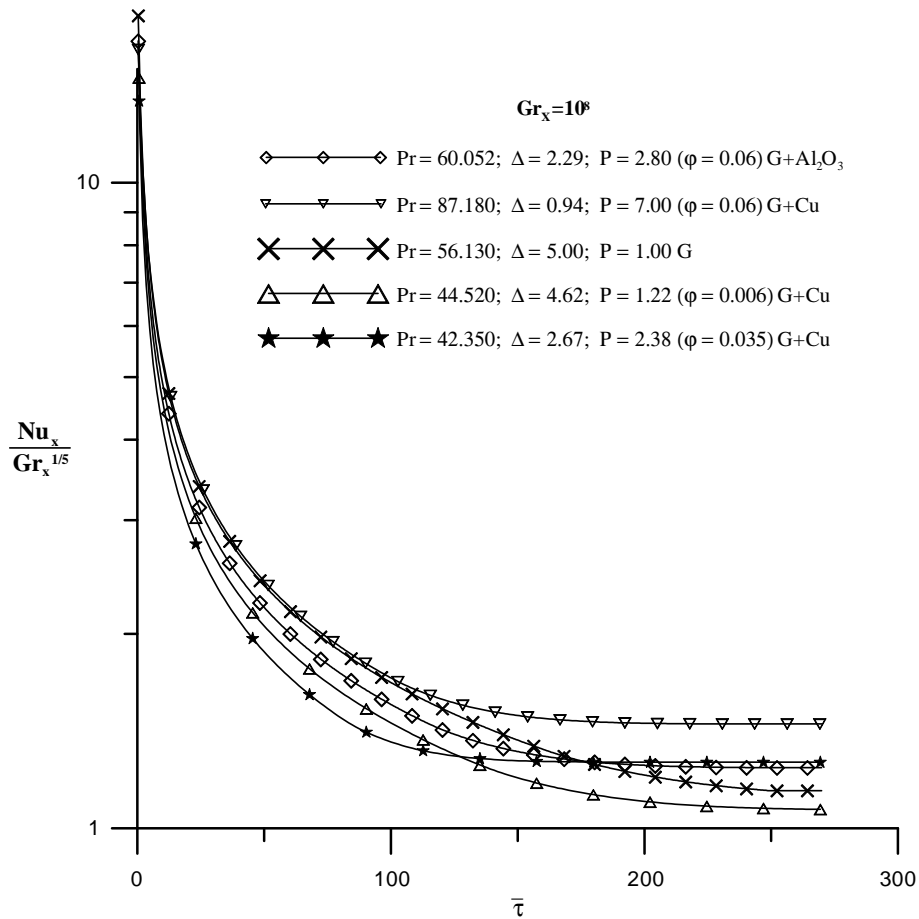


FIG. 4. Transient changes of the local Nusselt number.

The relationship (5.2) is shown graphically in Fig. 4. For the sake of comparison, Fig. 4 comprises the corresponding curve obtained for the selected values of parameters  $Pr_\infty$ ,  $P$ ,  $\Delta$ . The values of  $\Delta$  and  $P$  from Table 2 result from the assumption based on [5, 7, 8], which indicates the parameters of fluids without nanoparticles. In particular, the values of  $\Delta$ : 5.0, 2.29, 0.94 etc. result from the conversion of characteristic values describing the physical properties of fluids without nanoparticles to values describing fluids with nanoparticles. It is worth mentioning that with an increase of the nanoparticle volume fraction in the ethylene glycol solution, the Prandtl number decreased in comparison with pure ethylene glycol. Also, for the volume fraction greater than about 4%, the Prandtl number increases according to the equations presented in [4]. The presented calculation shows that the decrease in the parameter  $\Delta$  increases the intensity of the heat transfer in comparison with changes in  $P$  parameter.

Curves in Fig. 4 represent the local Nusselt number with respect to the local Grashof number  $(Nu_x/(Gr_x)^{1/5})$  specific to the value  $Gr_x = 10^8$ . It is worth mentioning that the corresponding lines of parameter  $(Nu_x/(Gr_x)^{1/5})$  have a different dimensionless  $X$  coordinate. For pure ethylene glycol, the coordinate  $X = X_f = 100$  corresponds, due to equations (3.17) and (3.18), to Grashof num-

**Table 2. A comparison of results.**

$Pr_\infty$	$\Delta$	$P$	$(Nu_x/(Gr_x)^{1/5})$	$\bar{\tau}_w$
56.310 G	0.0	0.0	1.3795*	0.16189*
	0.0	0.0	1.4117	0.15302
	5.0	1.0	1.1311	0.0691
60.052 G+Al <sub>2</sub> O <sub>3</sub> (38.4 nm) $\varphi = 6\%$	0.0	0.0	1.39844*	0.15778*
	0.0	0.0	1.4351	0.14886
	2.290	2.798	1.2402	0.09164
87.180 G + Cu (10 nm) $\varphi = 6\%$	0.0	0.0	1.5126*	0.13592*
	0.0	0.0	1.5632	0.12753
	0.940	6.999	1.45053	0.09924
44.520 G + Cu (10 nm) $\varphi = 0.6\%$	4.62	1.22	1.0696	0.07946
42.350 G + Cu (10 nm) $\varphi = 3.5\%$	2.67	2.38	1.2658	0.08000

ber  $Gr_x = 10^8$ . For the same Grashof number, the dimensionless coordinate  $X$  is respectively for nanofluids  $X_{Al_2O_3} = 0.598X_f$  and  $X_{Cu} = 0.378X_f$ . As indicated in Fig. 4, the intensity of the heat exchange in micropolar nanofluid is significantly lower than in corresponding nanofluids. On the basis of the calculated velocity field, a shear stress on the vertical plate was determined. Taking into account the constitutive equations for micropolar nanofluids [6]–[8] we obtain:

$$(5.4) \quad \tau_w = \left[ (\mu_v + \kappa_v) \frac{\partial u}{\partial y} + \kappa_v \mathbf{v}_r^{(z)} \right]_{|y=0}.$$

After adding dimensionless equations (3.15)–(3.19) to the above equation (5.4) we obtain:

$$(5.5) \quad \bar{\tau}_w = \frac{\tau_w}{\frac{\rho_\infty \nu_\infty^2}{x^2} 5^{2/5} Gr_x^{3/5} (1 + \Delta - n\Delta)} = \frac{1}{(5X)^{2/5}} \frac{\partial U}{\partial Y} \Big|_{y=0}.$$

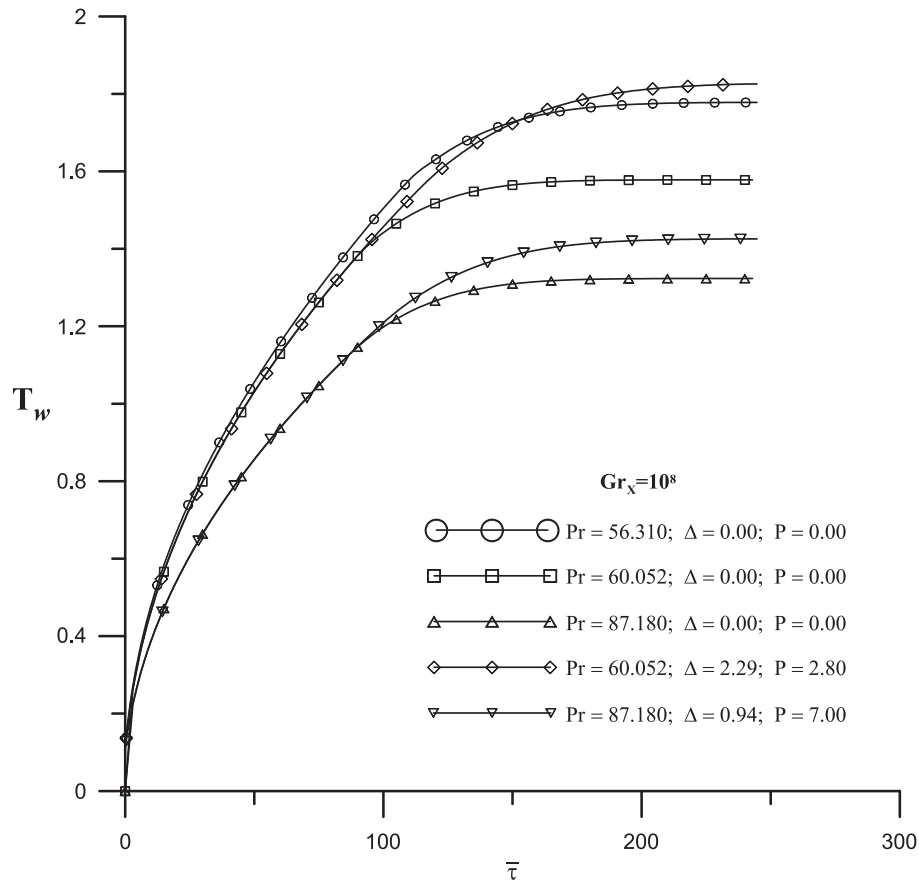


FIG. 5. Transient changes in dimensionless temperature on vertical plate.

In order to make a comparative analysis, Table 2 summarizes: the Nusselt number values according to the (5.2) formula and the dimensionless shear stress in accordance with the (5.5) formula, obtained from the numerical calculations performed for the variable parameters  $\Delta$ ,  $P$ ,  $Pr_\infty$  and the constant  $n$  parameter ( $n = 0.5$ ). The summarized results relate to the steady state with the Grashof number  $10^8$ , which is reached for nanofluid when the dimensionless coordinate  $X$  is lower than the  $X$  coordinate for pure ethylene glycol ( $X_f = 100$ ). This coordinate is measured along the vertical plate. The exact values of quotient  $X/X_f$  and  $Y/Y_f$  (Table 1) according to the relationships (2.1), (2.7), (2.9), (2.10), (3.16) take into account the respective values of the thermophysical parameters of pure ethylene glycol and considered nanofluids. In Table 2, the values with \* were taken from [10]. The result from [10] was calculated with the exact analytical solution of conservation equations for a Newtonian fluid.

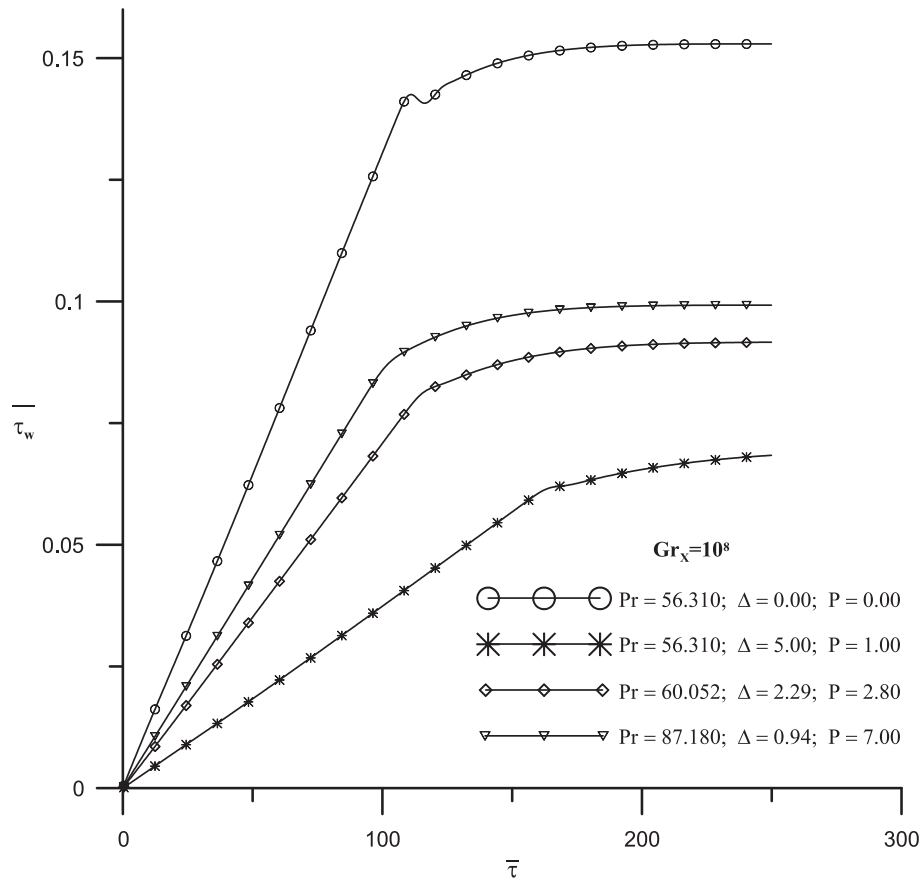


FIG. 6. Transient changes in dimensionless shear stress on vertical plate.

Figure 5 shows changes in the vertical plate temperature heated with constant heat flux  $q_0$ . Due to the high value of the Prandtl number of the analyzed fluids, the fixed temperature values are reached after time  $\bar{\tau} > 200$ . The steady state temperature value distinctly depends on the micropolar properties of analyzed nanofluids. With the higher value of a  $\Delta$  parameter, the temperature of vertical plate reaches a higher value at the end of the process.

The dimensionless shear stress component on the vertical plate, according to equation (5.5), is presented in Fig. 6. This shear stress component ( $\bar{\tau}_w$ ) depends on the parameters describing the micropolar properties of nanofluid near the vertical plate. The constant values of shear stress are reached in the steady state for dimensionless time  $\bar{\tau} > 200$ .

Figure 7 presents the dimensionless component profiles of microrotation in selected moments of the heating process. The greatest microrotation changes

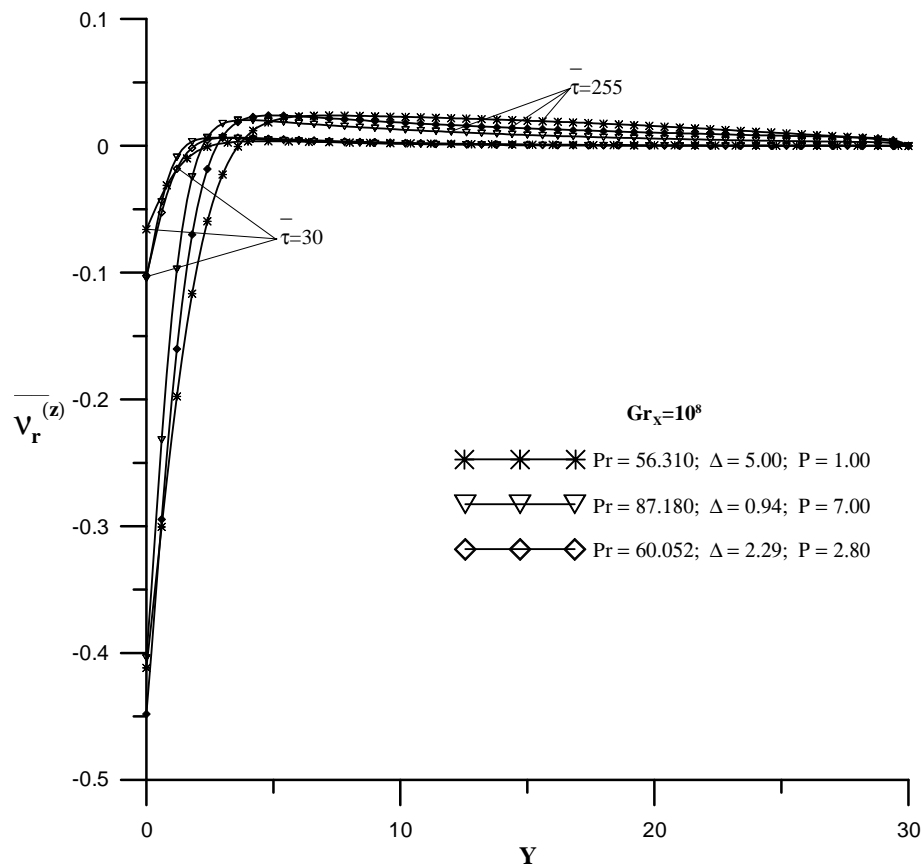


FIG. 7. The changes in the profiles of dimensionless microrotation at certain moments of the process.

**Table 3. A comparison of results.**

Fluid	$\Delta$	P	$(Nu_x/(Gr_x)^{1/5})$	E [%]
G	0.0	0.0	1.4117 <sub>f</sub>	-
G + Al <sub>2</sub> O <sub>3</sub> (38.4 nm), $\varphi = 6\%$	0.0	0.0	1.4351	1.66
G + Cu (10 nm), $\varphi = 6\%$	0.0	0.0	1.5632	10.7
G (micropolar)	5.0	1.0	1.1311 <sub>f</sub>	-
G + Al <sub>2</sub> O <sub>3</sub> (38.4 nm), $\varphi = 6\%$	2.290	2.792	1.2502	9.6
G + Cu (10 nm), $\varphi = 6\%$	0.94	6.999	1.45053	28.2
G + Cu (10 nm), $\varphi = 0.6\%$	4.62	1.22	1.0696	-5.4
G + Cu (10 nm), $\varphi = 3.5\%$	2.67	2.38	1.2658	11.9

are observed in the analyzed nanofluids in the vicinity of vertical plate ( $Y < 5$ ) heated with constant heat flux  $q_0$ . Additionally, in order to obtain an unambiguous description, profiles of the dimensionless microrotation obtained for the time  $\bar{\tau} = 255$  are marked with black symbols.

Heat transfer enhancement during the natural convection in the considered nanofluids is represented by the following equation:

$$(5.6) \quad E = \frac{\frac{Nu_x}{Gr_x^{1/5}}}{\left. \frac{Nu_x}{Gr_x^{1/5}} \right|_f} - 1.$$

Table 3 presents the values of the E parameters calculated with relationship (5.6) for the considered nanofluid in a stationary position case. While calculating these values, corresponding results from table (2) were used. The maximum value of the E parameter is for nanofluid with Cu nanoparticles with a mean diameter of 10 nm.

## 6. Concluding remarks

In this paper, a process of heat and momentum exchange during natural convection in nanofluids with micropolar properties was analyzed. To describe the analyzed phenomena of exchange, the equations of hydrodynamic and thermal boundary layer were used. It is worth noting that the coupled system of differential equations describing the analyzed exchange process also includes, in accordance with the boundary layer theory, a simplified equation for the microrotation component, arising from the angular momentum principle. In order to solve this problem, the method of finite difference was applied. The obtained results were presented in graphs and tables.

Parameter E describing heat transfer enhancement between the heated plate and the nanofluid shown in Table 3, appears to have a maximum value equal to 10.7%, which was obtained for the nanofluid with Cu nanoparticles with a mean diameter of 10 nm and parameters  $\Delta$  and P equal to zero. For the same fluid, a relative decrease of temperature of the heated vertical plate was  $\sigma_{Cu} = -19.8\%$  at the end of the analyzed process in time  $\bar{\tau} = 255$ . The presented calculation shows that the largest increase in the intensity of the heat transfer occurs for ethylene glycol, based nanofluid with Cu nanoparticles with a volume fraction greater than 3.5%.

Micropolar fluids are fluids with non-zero values of  $\Delta$  and P parameters. These fluids are characterized by different behavior during natural convection. The calculation results obtained in this work for fluids with parameters  $\Delta = 5.0$  and  $P = 1.0$  show that dimensionless shear stress for micropolar fluids on a heated plate has lower values than the corresponding values for Newtonian fluid during entire process of heating. The maximal relative change of  $\bar{\tau}_w$  is equal to 57.3% ( $\Delta = 5.0$ ,  $P = 1.0$ ) and the maximal relative change of  $(Nu_x/(Gr_x)^{1/5})$  for micropolar fluid with respect to the Newtonian fluid equals 18.0%.

The significantly higher temperature value of the heated plate after time  $\bar{\tau} > 150$  in the vicinity of micropolar fluid indicates lower intensity of heat transfer by the analyzed micropolar fluid compared to the Newtonian fluid.

The highest changes in the microrotation component are observed in the vicinity of the vertical plate ( $Y < 5$ ).

In order to perform a comparative analysis of the results presented in this work, the exact result for Newtonian fluids was quoted from the literature.

## References

1. C. POPA, S. FOHANNON, C.T. NGUYEN, G. POLIDORI, *On heat transfer in external natural convection flows using two nanofluids*, International Journal of Thermal Science, **49**, 901–908, 2010.
2. G. POLIDORI, S. FOHANNON, C.T. NGUYEN, *A note on heat transfer modeling of Newtonian nanofluids in laminar free convection*, International Journal of Thermal Science, **46**, 739–744, 2007.
3. O. ABUALI, G. AHMADI, *Computer simulations of natural convection of single phase nanofluids in simple enclosures: A critical review*, Applied Thermal Engineering, **36**, 1–13, 2012.
4. M. CORICONE, *Empirical correlating equations for predicting the effective thermal conductivity and dynamic viscosity of nanofluids*, Energy Conversion and Management, **52**, 789–793, 2011.
5. S. KAKAÇ, A. PRAMUANJAROENKIJ, *Review of convective heat transfer enhancement with nanofluids*, International Journal of Heat and Mass Transfer, **52**, 3187–3196, 2009.

6. A.C. ERINGEN, *Theory of micropolar fluids*, Journal of Mathematics and Mechanics, **16**, 1–18, 1966.
7. A.A. MOHAMMEDAN, R.S.R. GORLA, *Heat transfer in a micropolar fluid over a stretching sheet with viscous dissipation and internal heat generation*, International Journal of Numerical Methods for Heat and Fluid Flow, **11**, 1, 50–58, 2001.
8. K. RUP, A. DRÓZDŹ, *The effect of reduced heat transfer in micropolar fluid in natural convection*, Archives of Thermodynamics, **34**, 45–59, 2013.
9. J.C. TANNEHILL, A.D. ANDERSON, R.H. PLETCHER, *Computational Fluid Mechanics and Heat Transfer*, Taylor & Francis, Washington, 1997.
10. O.G. MARTYNYENKO, J.A. SOKOWISKYN, *Heat transfer enhancement in natural convection in micropolar nanofluids*, Nauka, Minsk, 1977 [in Russian].

*Received September 14, 2015; accepted May 12, 2016.*

---